Residual stress generation in metal matrix composites (MMCs) after cooling

Choo Siew Wong[1], A. Pramanik*[1], A.K. Basak[2]

[1]Department of Mechanical Engineering, Curtin University, Bentley, WA 6102, Australia

[2]Adelaide Microscopy, University of Adelaide, Adelaide, SA, Australia

*Corresponding author, Email: alokesh.pramanik@curtin.edu.au, Fax: +61 (0)892662681, Phone: +61 (0)8 92667981.

Abstract

Effects of reinforcements' shapes, sizes and contents on (a) von-Mises stress along horizontal line in MMCs, (b) directions and distributions of principal stresses inside particles, matrix and interface, and (c) distribution of thermal residual stress in MMCs were analysed in this investigation. It was found that the matrix-particle interfaces experience sudden change of von-Mises stress which depends on the reinforcement shape. The smoothest change of stress was occurred in triangle particle reinforced MMCs. However, the highest stress was concentrated was at the corners of the triangular particles. The directions of stress vectors depend on the shape of the particles. The extent of the von-Mises stress increases with the increase of reinforcement content and decrease of particles size at constant content.

Key words: MMCs; particles shape; particle size; thermal stress.

1. Introduction

Metal matrix composites (MMCs) are a class of engineering materials that exhibits considerable advantages over conventional monolithic materials including excellent corrosion resistance, wear resistance, improved strength and stiffness, high electrical and thermal conductivity and outstanding creep resistance (1). These are some properties that are essential for the materials to be considered for number of structural applications such as drive shafts, bicycle frames, brake disks, diesel engine pistons and suspension components for vehicles and heavy industrial equipment (2). MMCs were developed to fulfil the ever increasing challenges of modern technologies as well as to overcome the limitations of conventional materials' properties (3). Reinforcements in MMCs may be discontinuous i.e., in the form of short fibres, whiskers or particulates; or continuous i.e., in the form of long fibres. Kaczmar et al. (4) investigated the properties of MMCs reinforced with long and short fibres, platelets as well as particles and reported that, particle-reinforced MMCs particularly aluminium matrix reinforced with silicon carbide exhibit some favourable properties in structural applications such as automobile and aerospace industries. These properties include high specific strength and stiffness, high wear resistance and isotropic mechanical properties. Particle-reinforced MMCs are relatively inexpensive to fabricate due to lower material and production costs and easy to design compared to the alternatives such as advanced alloys and fibre reinforced MMCs (5, 6). However, in spite of all the advantages compared to other materials, there is a major concern regarding MMCs which is still under investigation. This is regarding to

thermal residual stresses that occur in MMCs due to mismatch in thermal expansion of the matrix and the reinforcements (7). Residual stresses, which are also referred as locked-in stresses or internal stresses, exist in a body without the application of external forces. These stresses develop during cooling after thermomechanical treatment or fabrication and may significantly affect the behaviours of materials. Manufacturing operations such as heat treatment, surface hardening and welding induced residual stresses in the workpiece. For instance, machining operations, which are chip-removal processes (i.e., grinding and turning), lead to mechanically induced residual stresses in the material (8). Residual stresses that are thermally induced in the material due to heat treatment are also known as thermal residual stresses. Thermal residual stresses can arise when the MMCs with different constituent phases are subjected to temperature changes (9).

Ho et al., (10) used thermo-elastoplastic finite element analysis (FEA) to investigate the thermal residual stresses induced in 20 µm SiC reinforced aluminium A357 matrix composite during casting and subjected to various cooling rate such as water, air and constant temperature cooling. It was noted that, the matrix experiences significant plastic deformation during the cooling process and the highest residual stress occurs at matrix/particle interface. Higher cooling rate as well as higher volume fraction of particles induce higher residual stress in the matrix. Povirk et al., (11) analysed the residual thermal stresses generation in SiC whisker reinforced aluminium MMCs with different aspect ratio (2, 4 and 8) and varied volume fraction (10%, 20% and 30%) of reinforcements by using FEA. They found insignificant effect aspect ratio on the magnitude or distribution of effective plastic strain in the matrix where the side-to-side spacing of fibres was the most important parameter that controlled the residual stresses and intensity of plastic deformation. The induced plastic strains increased with the increase of spacing among the fibres. The distribution and magnitude of thermal residual stress in SiC reinforced aluminium MMCs using finite element method was also investigated by Bouafia et al., (2) who varied particle volume fraction, particle spacing and particle shape while keeping particle diameter (10 µm) constant. They found that an increase in particle volume fraction increase the thermal residual stresses in matrix, where the thermal residual stresses pertaining to the particles decrease with increasing volume fraction. Therefore, there is a risk of crack initiation in the regions of highly concentrated particles provided the particles are not homogenously distributed in the matrix. Similar results were obtained by Teixeira-Dias and Menezes (12) for aluminium MMCs reinforced with spherical, cylindrical and cubic shaped particles using numerical approach. Intense residual stress around pointed corners of angular particles was noted where the stress concentration increase with the increase of the sharpness of particle corners. The maximum von-Mises residual stress in the shuttle-shaped particle reinforced composite was higher than that of spherical particles.

Though there are considerable amount of researches have been reported on thermal residual stress generation, however, most of the researches consider a limited number of variables as well as variation of variables. Distribution, direction and magnitude of residual stresses were rarely investigated in details while varying shapes, sizes and contents of reinforced particles. These factors are considerably important for better

understanding of MMCs for proper applications. This research modelled and studied the effects of reinforcements on thermal residual stress in MMCs with four different reinforcement particle geometries (circle, equilateral triangle, square and rectangle) and each geometry had three different contents and sizes. The von Mises residual stress distribution and the stress vector directions surrounding the reinforcement particles were demonstrated and investigated. The residual stress generated in composites with varied sizes, shapes and contents of reinforcement particles were compared with each other. The results of this research provide reliable data about effects of inclusions on thermal stress generated during cooling process to further improve the mechanical properties of MMCs and minimise the detriment of thermal residual stress.

2. Finite element modelling

Numerical techniques, such as finite element analysis (FEA) were developed as an analytical methods and can be difficult to deal with composite systems that involve non-homogeneous deformation due to matrix plasticity and comprises multiple reinforcement with sharp corners. Withstanding its above mentioned challenge, FEA has been widely used by researchers to predict the constitutive responses of MMCs and associated residual stresses (13-16). Thirty-six cases with varied shapes, sizes and contents of reinforcement particles were modelled using the finite element analysis software, ANSYS in this research. The size of MMC model blocks remain constant throughout the simulation for the ease of comparison of the results. Circular, triangular, square and rectangular shape reinforcements with different sizes and volume contents (i.e., 10%, 15% and 20%) were considered in this analysis where the number of particles varied in specific area as given in table 1. Therefore, nine study cases in total were established for MMCs reinforced with each particle shape. All the reinforcement particles were distributed homogeneously in the finite element for better judgement about the effects of size, shape and content. The area of reinforcement particles remained constant for square, rectangular and equilateral triangle, as per the area of circular particles. Thus, the area of each shape was the same but varied in perimeter. The length of the sides for square, rectangle and equilateral triangle were calculated accordingly and tabulated as shown in Table 1. The aspect ratio of rectangular reinforcement particles was selected as 1:3.

The dimension of MMC model block was calculated to contain an integer number of particles in each study case so that an exact required volume percentage of the reinforcement particles could be obtain easily. The area of MMC model block required was calculated as 27,143 μm^2 and based on the length to width ratio of 1:4, were 329.5 μm and 82.4 μm respectively.

Table 1: Sizes and number of particles.

Reinforcement content (vol.)	Diameter of circle shape (μm)			Sides of square shape (μm)			Sides of equilateral triangle shape (μm)			Short sides of rectangle shape (μm)		
	6	12	24	5.3	10.6	21.3	8.1	16.2	32.3	3.1	6.1	12.3
	Number of particles in the model block											
10 %	96	24	6	96	24	6	96	24	6	96	24	6
15 %	144	36	9	144	36	9	144	36	9	114	36	9
20 %	192	48	12	192	48	12	19	48	12	192	48	12

In this research, the MMC work material was a 6061-aluminium alloy reinforced with silicon carbide particles. Al 6061 is a precipitation-hardened aluminium alloy exhibits relatively high strength and excellent thermal conductivity. On the other hand, silicon carbide, as a compound of silicon and carbon, is extremely hard. It also has high thermal conductivity, low thermal expansion and high-temperature strength. This particulate reinforcement was considered as a linear isotropic material, which means that its properties are independent of direction. Table 2 represents the material properties for 6061 aluminium alloy and silicon carbide. The stress strain curve of Al 6061 and silicon carbide are also shown in Fig. 1.

Table 2: Properties of 6061 aluminium alloy and silicon carbide (17, 18).

Material	Thermal conductivity ($Wm^{-1}K^{-1}$)	Heat capacity ($Jkg^{-1}K^{-1}$)	Density (kgm^{-3})	Thermal expansion ($10^{-6}\ K^{-1}$)	Young's modulus (GPa)	Poisson's ratio
Al 6061	167	896	2700	25.2	68.9	0.33
SiC	120	750	3100	4.0	410	0.14

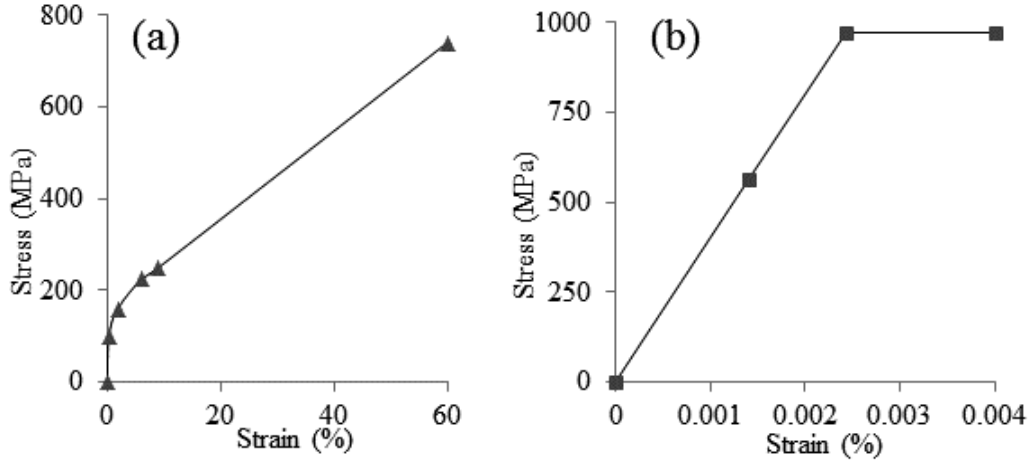

Fig. 1: Stress versus strain curve for (a) aluminium alloy and (b) silicon carbide particle (1).

Thermal solid Plane 77 (8 node) and structural solid Plane 183 (8 node) elements for 2D thermal and structural analysis were used respectively in this investigation. The reinforcement particles were perfectly bonded to the

matrix material. The MMC blocks were modelled and meshed with manual sizing and optimized to achieve the best convergence and accuracy of the results. The meshed MMC block with 10 % circular reinforcement particles is shown in figure 2. An initial temperature of 582 °C which is the melting point of 6061 aluminium matrix was applied on the blocks with surrounding temperature of 25 °C. The blocks were cooled down to room temperature and the thermal residual stresses generated during cooling process was investigated.

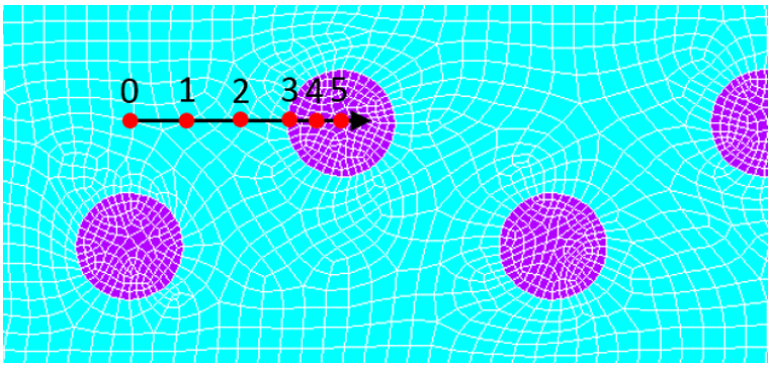

Fig. 2: Modelling and meshing of MMCs.

There is no basic rule in choosing these points. It was tried to clearly present the stress status in the matrix and particles. In doing so, the first reference point was taken at the interface, i.e., at point 3 (in Fig. 2) then the second point at the centroid of the particle, i.e., point 5 (in Fig. 2). The third point was at 0 in the matrix, which was in the middle of two particles in the horizontal direction. Due to symmetric nature of MMCs, the points 0 to 5 covered all aspects of the stress variation in matrix as well as in the particle. Points 1, 2 and 4 were considered to have more details along the line 0 to 5. For all the shapes, these lines were horizontal and went along the centroid of the particles. The line entered the square and triangle particles through the side arm. It entered rectangle shape through the long arm. The effect of different shape of particles was based on the identical area of particles regardless of shape.

3. Results

As shown in Fig. 2, thermal stresses at points 0 to 5 on a horizontal path through centroid of particles were considered for the analysis for all the case studies. The point 3 (in Fig. 2) got two perfectly bonded nodes, one of which from the materix material and the other from reinforcemnt patricle. These two nodes behave differently and provide a very important information on the generation of residual stress.

3.1 Effect of volume fraction of reinforced-particles on residual stress

Fig. 3 shows the stresses at points 0 to 5 from the matrix to particle with the variation of the contents for different sizes of circular particle. The point 0 which is furthest from the centre of the reinforcement got the smallest stress for all the cases. But the stress increases as the points are getting closer and the stress is

maximum in the matrix. The stress then drops very suddenly at point 3 in the reinforcement and continues to particle centre. This trend is very similar in every cases. It is noticed that, the stress at point 0 is maximum when the content of the reinforcement is maximum. But it is smallest at the interface in both materials and remain minimum in the side of the particles when compared with lower reinforcement contents. The highest stresses were noted in the particles with lowest reinforcement content. Therefore, the residual stress in the particle has an inverse relationship with the content of reinforcement, which means that residual stress in particles decrease with increasing reinforcement content. On the other hand, the stress level at the matrix side of matrix-particle interface also decrease with increasing reinforcement content but the difference of stress level due to reinforcement content is relatively insignificant.

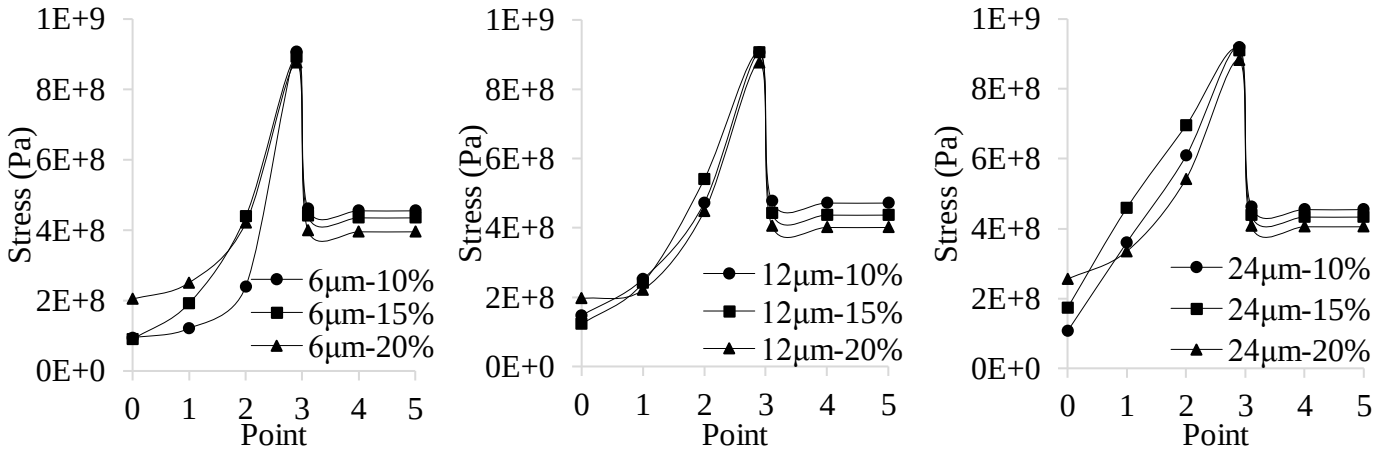

Fig. 3: Circular particles of 6, 12 and 24 µm diameter with different volume contents.

For square particles as shown in Fig. 4, the trend of stress field is similar with that of circular particles, which reaches the maximum at the matrix side of matrix-particle interface then decreases abruptly. However, the reduction of stress level in square particle across the boundary is not as much as in circular particle. The residual stress decreases slightly towards the centroid of particle. The residual stresses in the matrix increases and decreases in particles with the increase of reinforcement content. However, the difference of stress level is insignificant, especially at matrix-particle interface but becomes more distinct moving away from matrix-particle interfaces.

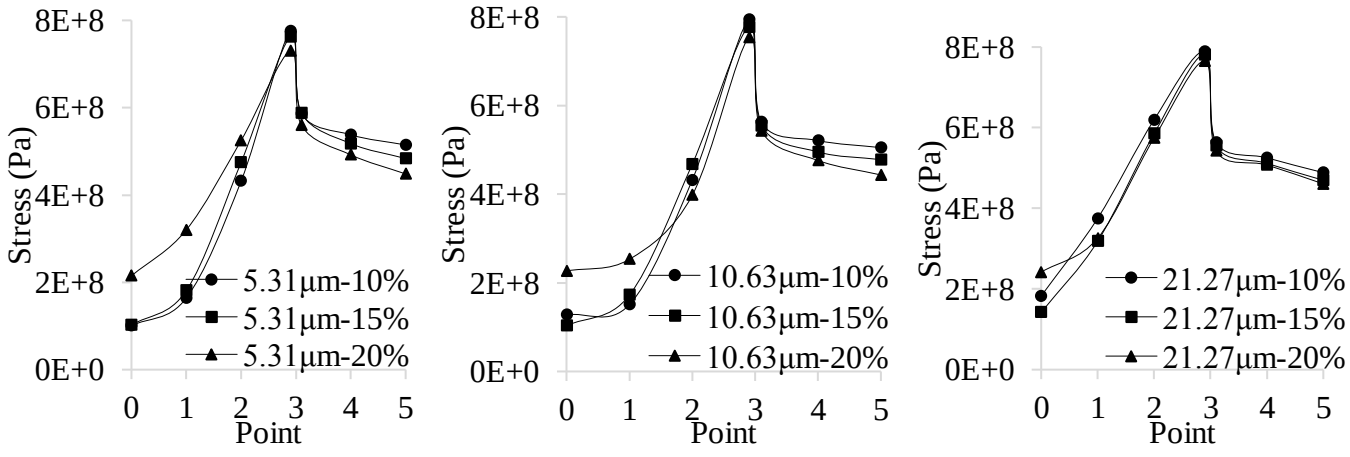

Fig. 4: Square particles with dimensions of 5.31, 10.63 and 21.27 μm with different volume contents.

For rectangle particles as presented in Fig. 5, unlike circular and square particles, an opposite behaviour was observe, that is, the stress increases abruptly and reaches its maximum once entering the particles. Then it decreases towards the centre of the reinforcement. The increment of stress depends largely on the reinforcement content. It increases more when the particle content is less. The stress in the centre of particles was minimum when reinforcement content is higher. No significant variation of stress was observe in the matrix of the matrix-particle interface with the variation of reinforcement content.

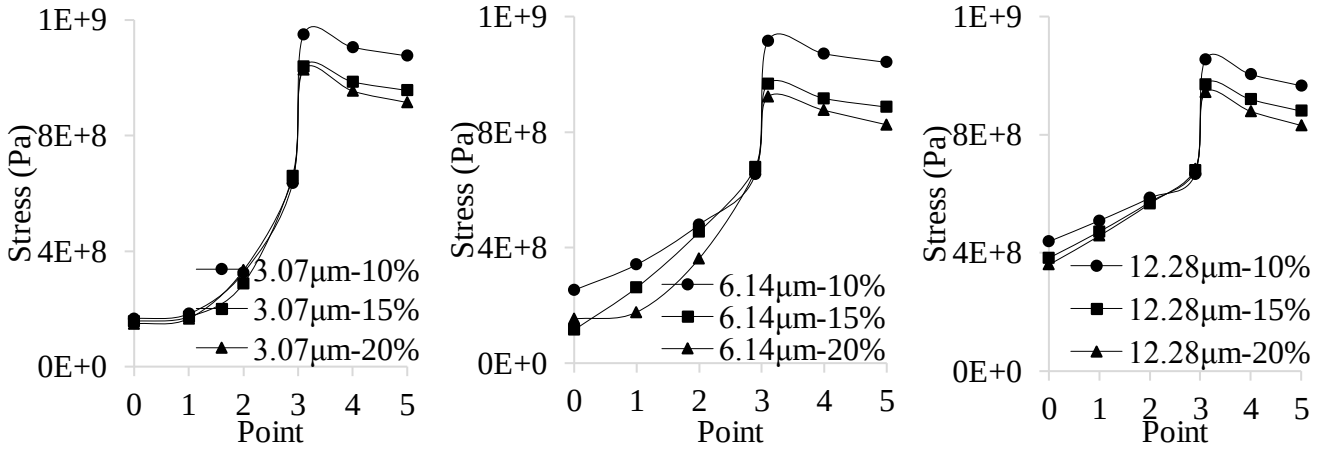

Fig. 5: Rectangle particles with dimensions of 3.07, 6.14 and 2.28 μm with different volume contents.

The stress variation along the horizontal line of triangular particle reinforced MMCs is shown in Fig. 6 and very similar to that of rectangle particle reinforced MMCs. The stress in the interface rises suddenly as moved from matrix material to reinforcement. The highest stress in the interface of the particle was noted at maximum reinforcement content. These stresses decrease toward the particle centre and the maximum stress in the centre was noted when the reinforcement content was maximum. The stress level at the centroid of triangle particles is much lower compared to that of at the interface. The highest stress in the matrix was developed at the furthest point from the interface at maximum reinforcement content.

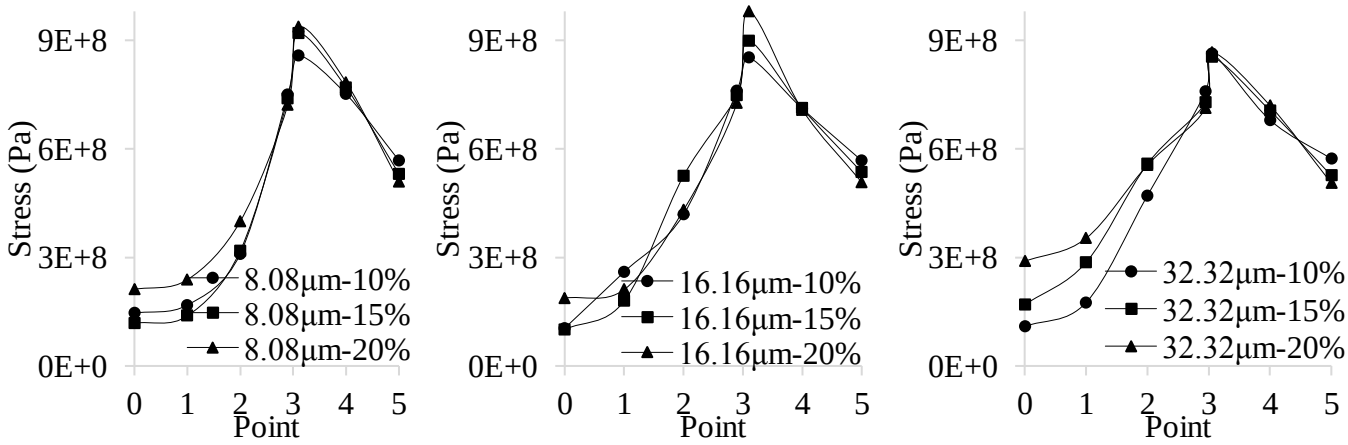

Fig. 6: Triangular particles with dimensions of 8.08, 16.16 and 32.32 μm with different volume contents.

3.2 Effect of reinforced-particles size on residual stress

The effect of reinforcement size on residual stress is analysed by keeping reinforcement content and geometry constant as shown in Figures 7 to 10. The stress in the matrix furthest from the interface is apparently higher when reinforcement size is bigger. Then the stresses increase at different rate depending on particle size and converge to a similar value as the distance from the interface decreases. For the circular particles as shown in Fig. 7, the stresses in the particle decrease suddenly at the interface and remain almost constant until the centre of the particles. Very similar trend of stresses along the horizontal line was also noted for square particles as shown in Fig. 8. However, in this case sudden decrease of stress at particle interface was smaller than that of circular shaped particles and decreases slightly towards the particle centre.

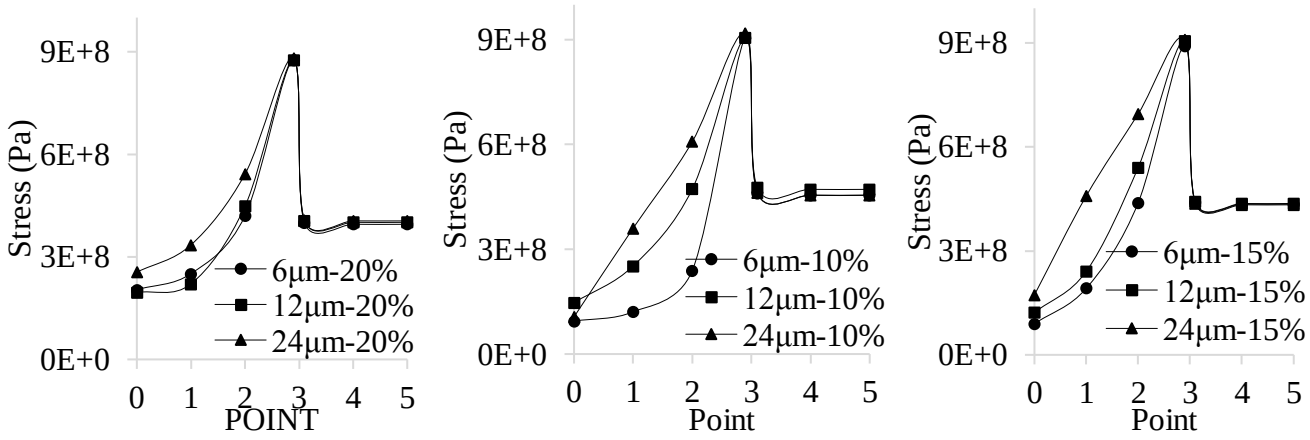

Fig. 7: Effect of size of circular particles with 10%, 15% and 20% contents

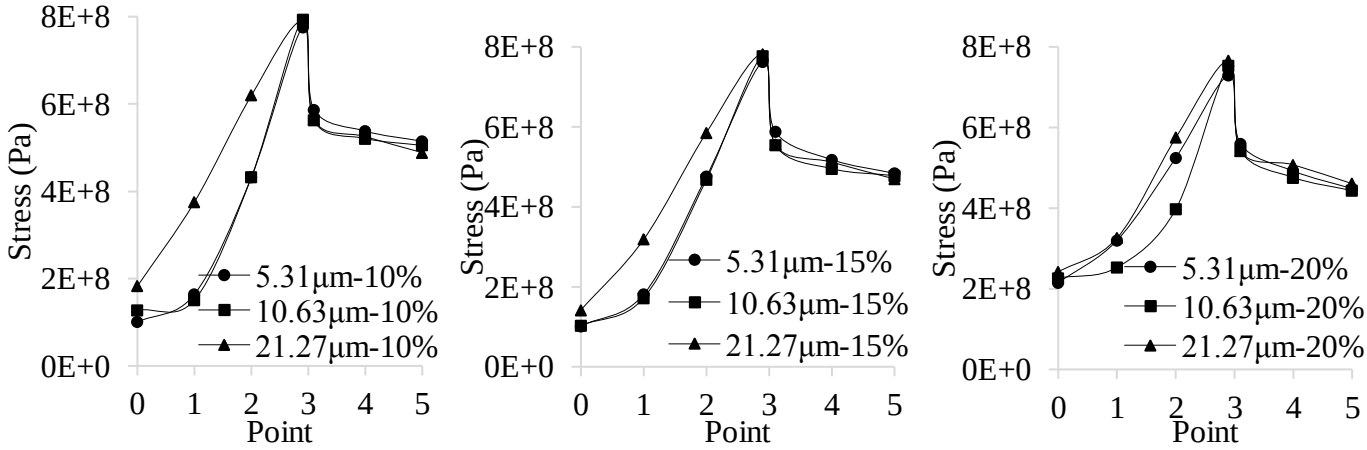

Fig. 8: Effect of size of square particles with 10, 15 and 20% contents.

The effect of size of rectangular particles on thermal stress is shown in Fig. 9. As mentioned earlier, the interface stresses in the particles increase suddenly and this increase depends on the size of the particles. The stress in MMC with the smallest particles increase most. The effect of particle size on interface stress for the

case of triangle particles is inconclusive as shown in Fig. 10. The increase of stress for all the size and content of triangle particles is smaller than that of square particles. When the particle content is 10 %, highest stress was occurred with largest particles. However, in case of 15 % content, highest stress occurred with medium size particle and for 20 % content it was for smallest particles. In all cases, the stresses in particles from the interface decrease at highest rate and converge towards the particle centroid whilst having the same stress level at the centroid.

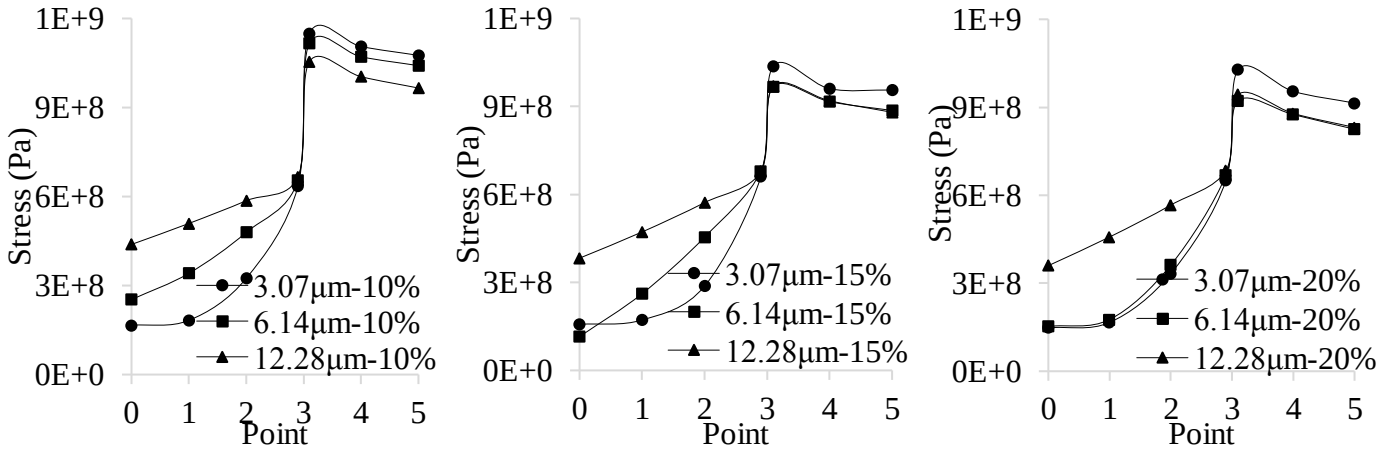

Fig. 9: Effect of size of rectangular particles with 10%, 15% and 20% contents.

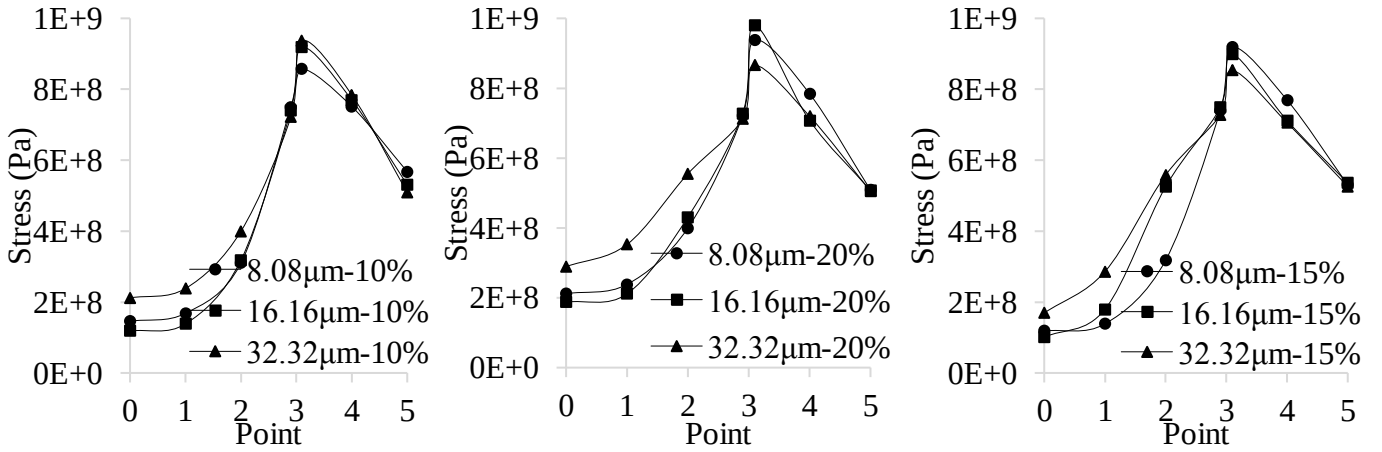

Fig. 10: Effect of size of triangular particles with 10%, 15% and 20% content.

3.3 Effect of reinforced-particles shape on residual stress

Figures 11 and 12 compare the effect of particle shape on residual stress for largest (20%) and smallest (10%) reinforcement contents respectively. The shapes of the markers in the stress lines represent the different shapes of reinforced particles considered in study, which is circular, rectangle, square and triangle. The trends of stresses with the variation of shapes are very similar irrespective of size and content of the reinforcements. As shown in Fig. 11, the difference of residual stress due to different geometry of particles at the furthest point from the interface is insignificant. Then the stresses increase towards the interface. At the matrix-particle

interface, the circular particles exert highest stress at the matrix, followed by triangle particles and square particles with relatively similar level of stress whilst rectangle particles have the lowest matrix stress at the boundary. On the other hand, the opposite pattern was observed for the stress in particles: rectangle particles have the highest inner stress, followed by triangle particles and square particles respectively; and circular particle have the lowest residual stress. The difference of stress level across the interface in triangle particles is the smallest followed by square, rectangle and circular particles.

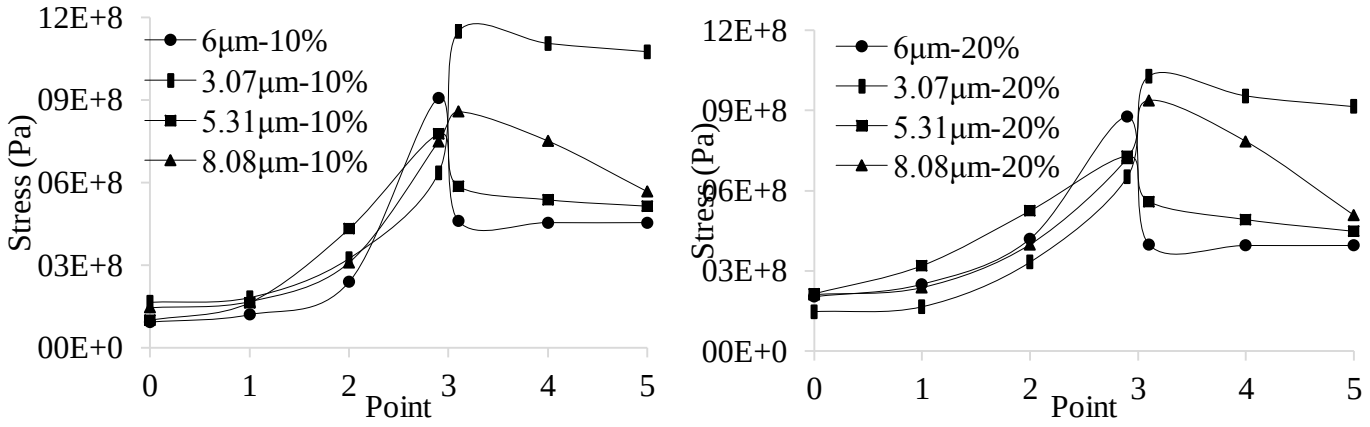

Fig. 11: Small particles with 10 and 20% contents.

When the particle size is bigger, the stresses in the matrix at point 0 depend on the shape of the reinforcements as shown in Fig. 12. The variation of the stresses at this point for 10 % reinforcement content is much higher than that of 20 % reinforcement content. However, in both cases the highest stresses at points 0 and 3 were generated for rectangular and circular particles, respectively. Similar to the case of small sized reinforced MMCs, the rectangle particles have the highest inner stress at the interface, followed by triangle particles and square particles whereas circular particle have the lowest residual stress. The difference of stress level across the interface in triangle particles is the smallest amongst all shapes, followed by square, rectangle and circular particles.

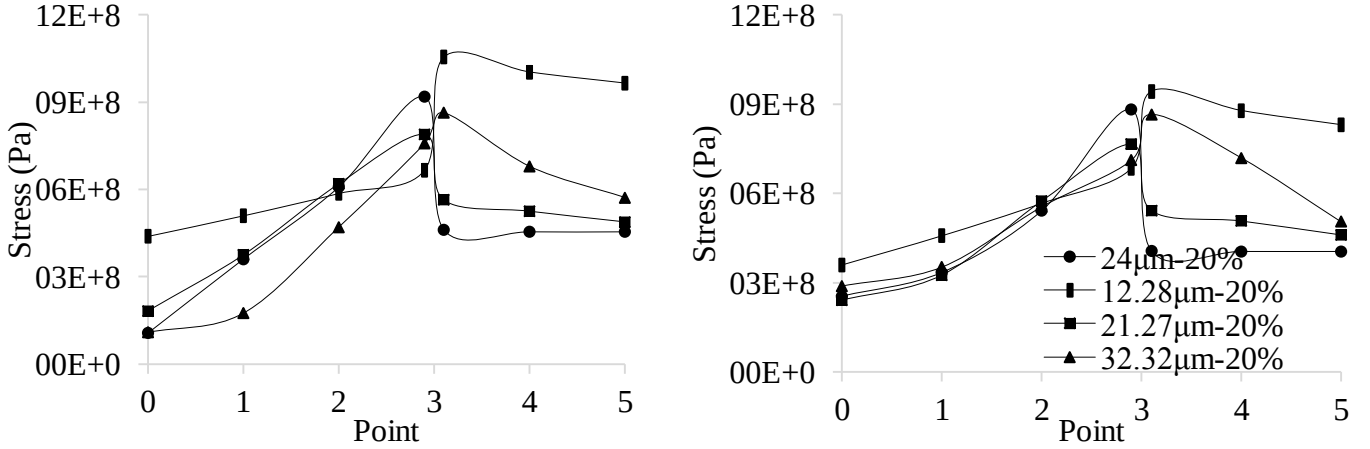

Fig. 12: Large particles with 10 and 20% contents.

The differences of residual stress level due to different particle geometry may be varied due to particle sizes and concentration. However, the effect of particle sizes is relatively insignificant compared to concentration. For instance, difference of residual stress in triangle particles and square particles at the matrix-particle interface is much higher in 20% content than in 10%, whether the particles are large or small.

The effect of reinforcement particles shape on thermal residual stress distribution is graphically represented shown in Fig. 13, using contour plot of different shape with same size and content (15%). For circular shaped particles, residual stress increases as getting closer to interface and reaches to a maximum at the matrix-particle interface followed by an abrupt decrease once entered the particle. The residual stress within the particle is distributed uniformly accress entire particle.

As for shapes with pointed corners such as rectangle, triangle and square particles, the residual stress concentrates at the corners. In rectangle shape, residual stress also increases towards particle-matrix interface as in circular shape. However, the stress increases abruptly as it passed matrix-particle interface, which is opposite to circular shape. Though the stress concentrated at four corners of the partiles, there are two low stress zones at the two ends of the particle.

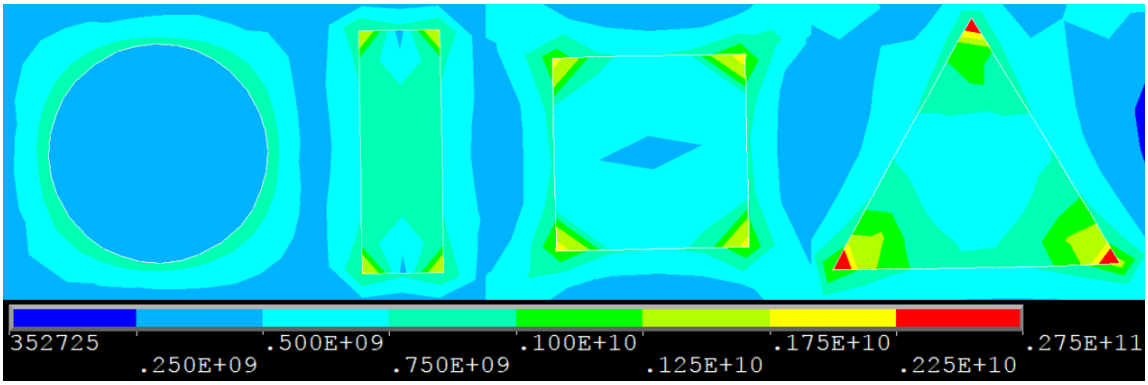

Fig. 13: Comparison of same size particles with 15% content.

The differences of stress distribution between square and rectangle shape mostly occur within the particles. The minimum residual stress is in square particle and concentrates at the centre whilst for rectangle particles it occurs at the middle point of short end of rectangle. This might be related to the variation in their aspect ratio. However, in regard to the stress distribution in the matrix around the particle, the difference is relatively insignificant. Within a relatively short distance from the corner of particles, the residual stress in matrix become independent of the axial coordinate.

The residual stress does not change significantly across matrix-particle interface at the mid area of each sides in triangle particle, unlike other shapes. However, stress difference increase towards the pointed corner and could be doubled the magnitude at the corner. In comparison, residual stress in the corners of triangle shape is the highest among the particle shapes considered in this investigation. The stress concentration in square particles is slightly higher than that of rectangle particles.

3.4 Magnitude based vector plot

The principal stresses in MMCs particles and surrounding matrix for different particle shapes are presented in Fig. 14. The first, second and third principal stresses are presented in white, green and blue arrows, respectively. The length and direction of the arrows represent the values and directions of the corresponding stresses. The magnitude based vector plots in Fig. 14 show that the stress in the particles is mainly compressive regardless of the shapes. The matrix in the particle-matrix interface experience compressive as well as tensile stresses. At this location, tensile stress is comparatively smaller than the compressive one. With the increase of distance from the interface, magnitudes of tensile stress increase and compressive stress reduces. Therefore, under general loading conditions MMCs are likely to fail in the matrix rather than at particle-matrix interface.

Each of the shapes show unique features in vector plot including directions and magnitude. The vector plot of circular particle shows radial direction of stress spreads evenly from the particles. The compressive stress is in radial direction along the interface in the particle as well as in the matrix. The tensile stress in the matrix is normal to that of the compressive stress. The stress vector field of rectangle particles takes the shape of magnetic field as shown in Fig. 14b. The matrix with square reinforcement shows a cross (‘X’) path of compressive stress in the matrix at the pointed corners, connecting to the pointed corners of neighbouring particles (Fig. 14c). As for triangle particles, compressive stress inside the particle acts in the direction of the pointed corner from the centroid of the triangular area (Fig. 16c). The compressive stress in this direction continues into the matrix around the pointed corners of the particles.

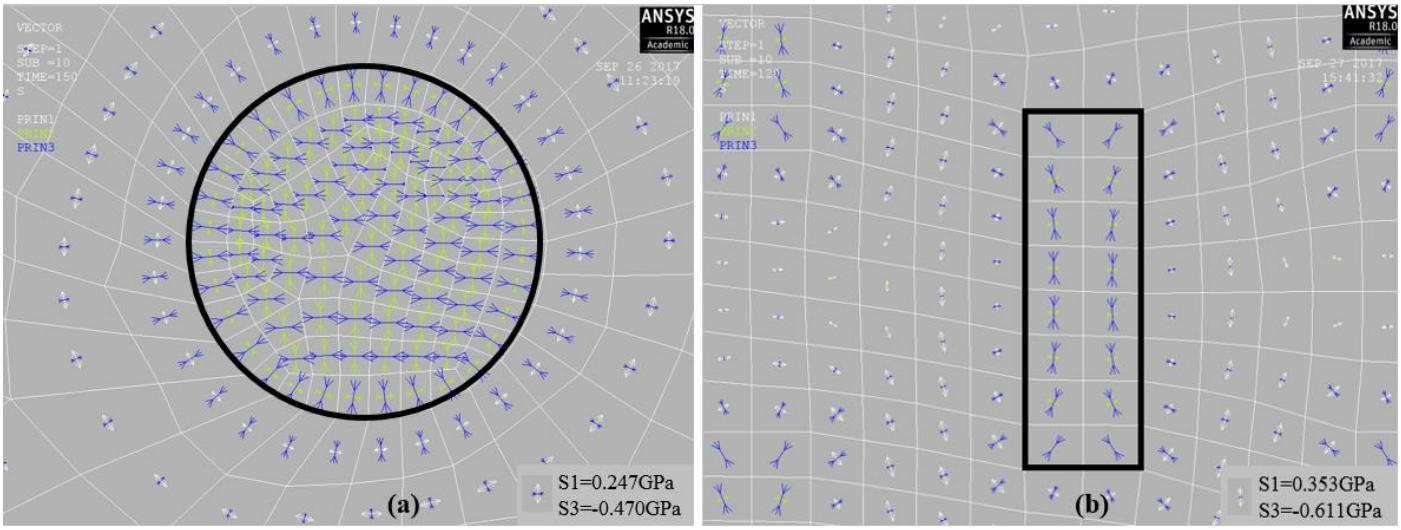

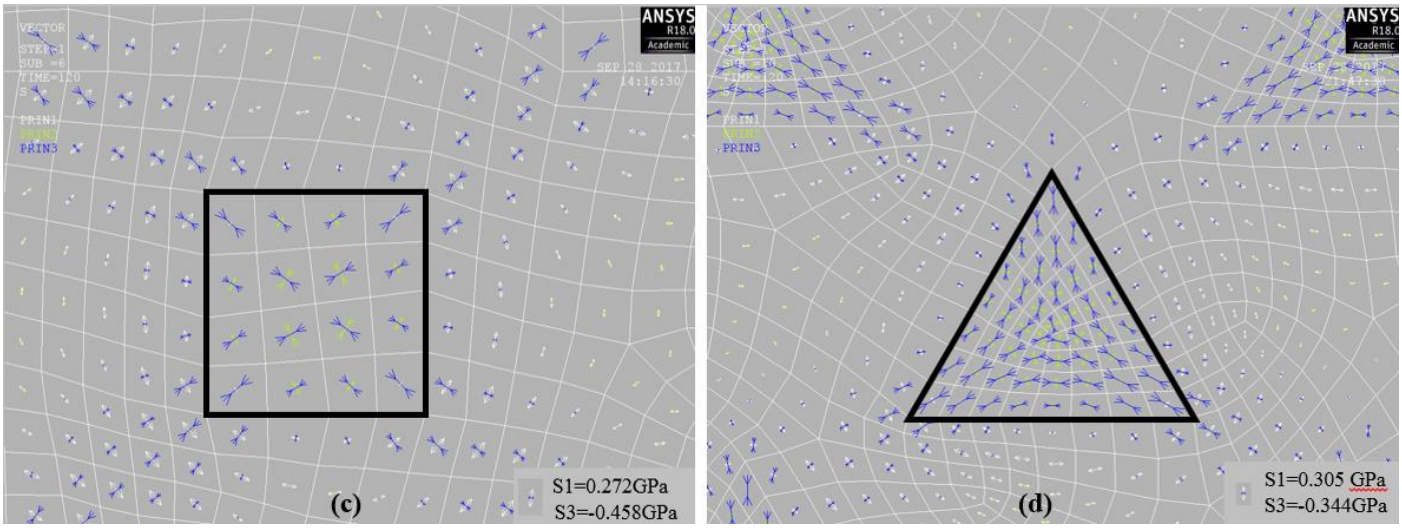

Fig. 14: Magnitude based vector plot for (a) circular, (b) rectangle, (c) square and (d) triangle particles with 15% content.

3.5 Stress distribution in MMC block

Figures 15-18 show the distribution and extent of Von-Mises stress in MMCs for all cases considered in this investigation. The stressed area in the matrix increases with the increase of reinforcement content as shown in the contour plot in the figures. The thermal residual stress in the matrix is highly localised at the vicinity of the particles as a result of decreased inter-particle spacing and results in an increase of average residual stress. When the size of the reinforcement decreases with constant reinforcement content, number of particles also increases, which reduces the inter-particle spacing. As mentioned earlier, effect of residual stress caused by reinforcement weakens in matrix material with increased distance from the particle. Therefore, the stress in the matrix extends and increases with the decrease of inter-particle spacing as expected.

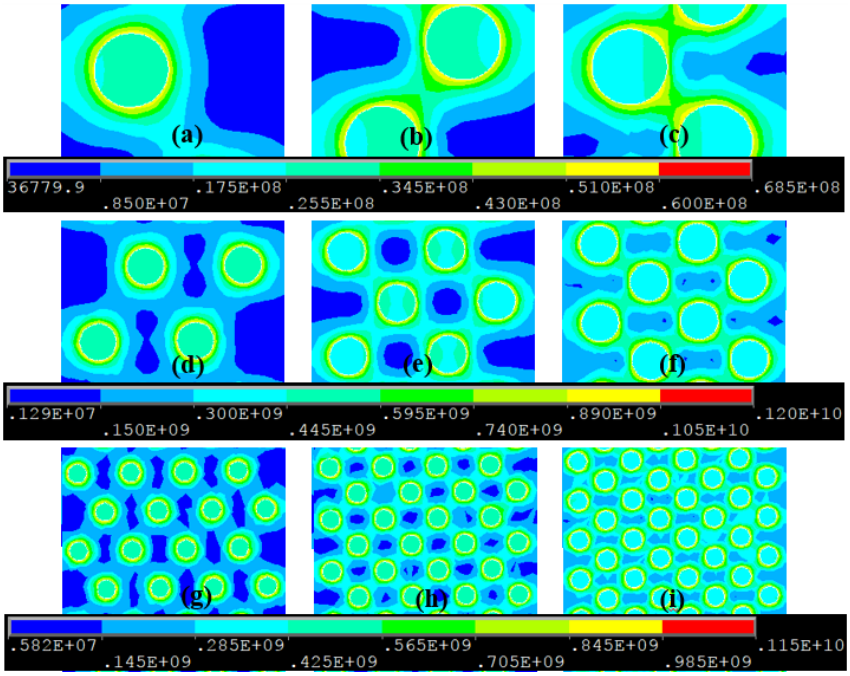

Fig. 15: Residual von-Mises stress in MMCs with circular particles of different sizes and contents: (a) 24 µm/10 %, (b) 24 µm/15 %, (c) 24 µm/20 %, (d) 12 µm/ 10 %, (e) 12 µm/15 %, (f) 12 µm/20 %, (g) 6 µm/10 %, (h) 6 µm/15 % and (i) 6 µm/20%.

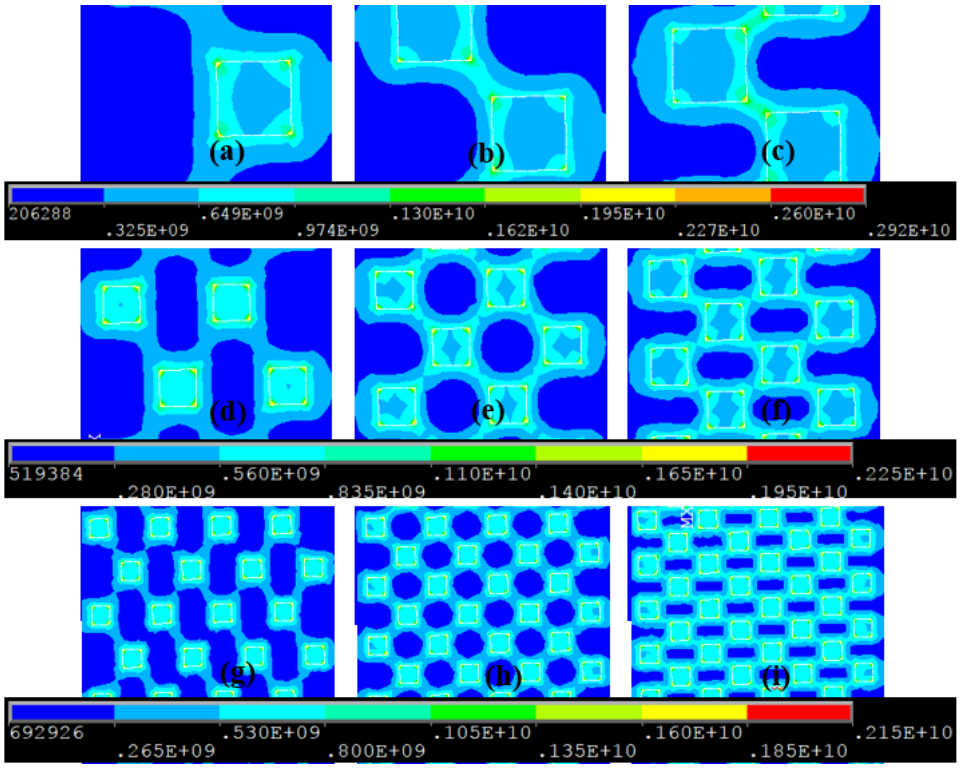

Fig. 16: Residual von-Mises stress in MMCs with square particles of different sizes and contents: (a) 21.27 µm/10 %, (b) 21.27 µm/15 %, (c) 21.27 µm/20 %, (d) 10.63 µm/10 %, (e) 10.63 µm/ 15 %, (f) 10.63 µm/20 %, (g) 5.31 µm/10 %, (h) 5.31 µm/15 % and (i) 5.31 µm/20 %.

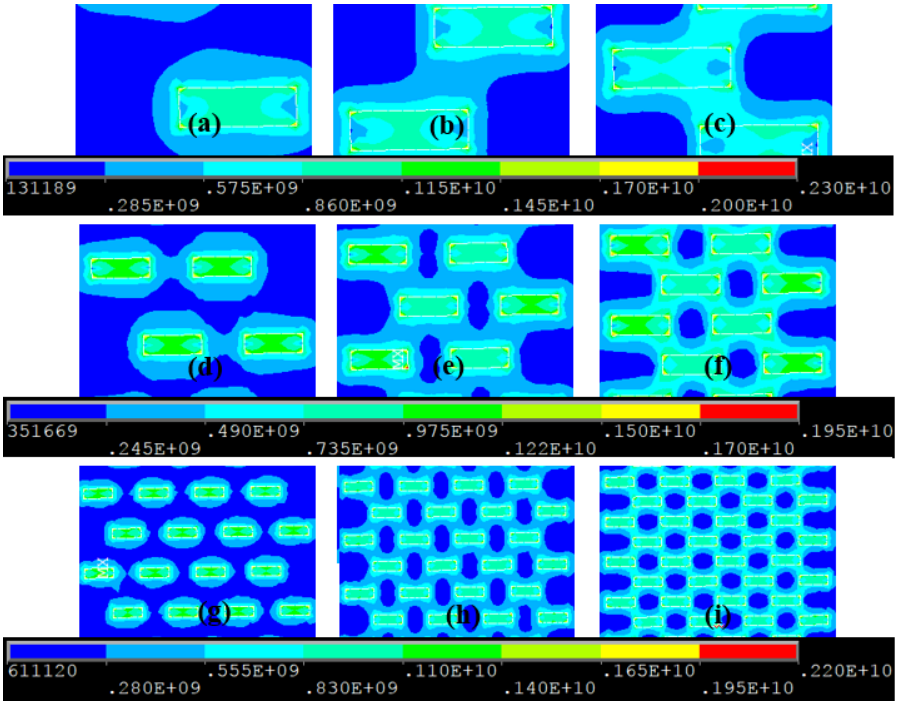

Fig. 17: Residual von-Mises stress in MMCs with rectangular particles of different sizes and contents: (a) 12.28 µm/10 %, (b) 12.28 µm/15 %, (c) 12.28 µm/20 %, (d) 6.14 µm/10 %, (e) 6.14 µm/ 15 %, (f) 6.14 µm/20 %, (g) 3.07 µm/10 % (h) 3.07 µm/15 % and (i) 3.07 µm/20 %.

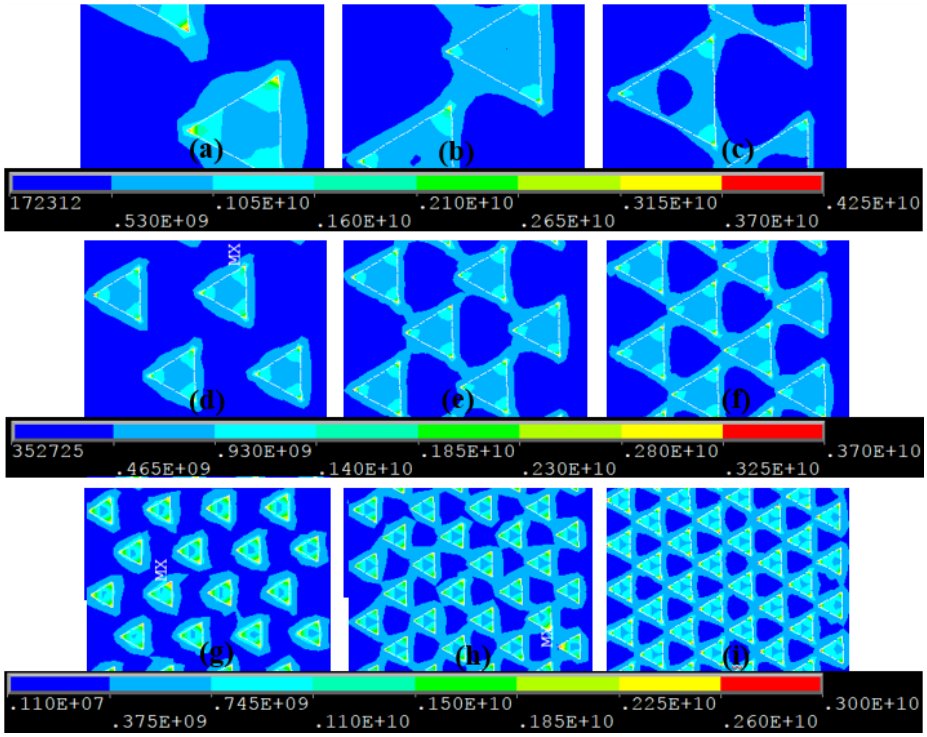

Fig. 18: Residual von-Mises stress in MMCs with triangular particles of different sizes and contents: (a) 32.32 µm/10 %, (b) 32.32 µm/15 %, (c) 32.32 µm/20 %, (d) 16.16µm/10 %, (e) 16.16 µm/15 %, (f) 16.16 µm/20 %, (g) 8.08 µm/10 %, (h) 8.08 µm/15 % and (i) 8.08 µm/20%.

A closer look in the contour plots indicates that the highest level of stresses were generated for triangular reinforcements and decreases in the order of rectangular, square and circular particles. For circular particles (Fig. 15) the maximum stress is localised uniformly in the interface for entire periphery. In this case, maximum stress significantly increases with the decrease of particle size and then it decreases slightly with further decrease of particle size. Maximum stresses were localised in the corner of particle when the shape is square as shown in Fig. 16 and decreases with the decrease of particle size for the range considered in this investigation. At certain combinations of size and shape, the stress distribution in circular particle reinforced MMCs and square particle reinforced MMCs are very similar as shown in Figures 15e and 16e; and 15h and 16h. The stress also concentrates in the corners of rectangle (Fig. 17) and triangle (Fig. 18) particles as does in square particles. Maximum stress initially decreases with the decrease of particle size then it increases with any further decrease of particles in the case of rectangular particles. However, the maximum stress in triangular reinforced MMCs decreases with the decrease particles size.

4. Discussion and validation of the results

Thermal residual stresses in composite materials, such as MMCs, are generated due to the differences in coefficients of thermal expansion (CTE) and elastic constants between matrix and reinforcement phases in composite materials. This occurs during cooling process from elevated fabrication temperature to room temperature. The level of expansion coefficient mismatch between matrix and reinforcement is directly related to the extent of residual stresses (19). Typical expansion coefficient of aluminium matrix is nearly five times higher than that of SiC reinforcement. On the other hand, elastic modulus of SiC reinforcement is apparently six time higher than that of aluminium matrix. Therefore, significant amount of residual stress is embodied naturally in MMCs during fabrication process as experimentally proved by Coats and Krawitz (20).

The Von-Mises stress in this analysis indicates the weaker locations on MMCs under thermal stress. The thermos-elastic stresses and strains induced by CTE mismatch are largest at matrix/reinforcement interface and decrease with distance from the interface. The reinforcements are in a state of hydrostatic stress that increases with increasing CTE, temperature change and elastic modulus. Matrix/reinforcement interface is a potential site for crack initiation under cycling thermal loading as plastic deformation initiated in the matrix adjacent to reinforcement particle (21). Particles having certain aspect ratio, such as rectangular and triangular shapes, is practically more realistic. It is not realistic to maintain circular or square shapes of the ceramics particles in micron level. It was noticed that rectangular and triangular particles got increased stress at the interface and that stress increase with the decrease of reinforcement content of rectangular particles. The similar results were experimentally obtained by Coats and Krawitz (20), Song et al., (22) and also reported by Bouafia et al., (2) based on finite element analysis.

Coats and Krawitz (20) found that the residual stresses in the reinforced particles and matrix are compressive and tensile respectively. They also noted that the size and content of reinforcement significantly affect thermal residual stress significantly. The mean thermal residual stress in the reinforcement decreases as the content and size increase. The thermal stress induces dislocation density which does not depend on other dislocation sources. This is caused by an activation of different slip systems in different areas (23).

Song et al., (22) investigated SiC/Al interfaces of different heat treated MMCs using transmission electron microscopy and found non-uniform dislocation distribution around the interface with regions of slightly different diffraction contrast as shown in figure 19. The presence of SiC/Al interfaces as well as the precipitates introduced by aging, may have given rise to substructure formation (i.e., the different diffraction contrast). During cooling from the high temperature processing of stir casting and extrusion deformation, the CTE mismatch between the particle and the matrix alloy is likely to cause residual stress in the vicinity of the interface (24), and subsequently a considerable increase in the dislocation punched zone size in the as-extruded and underaged samples. Thermal stress around the particles are high while the stresses away from the particles are low. Therefore, the interfacial region exhibits higher dislocation density than the rest of the matrix (25), which are shaded in figure 19.

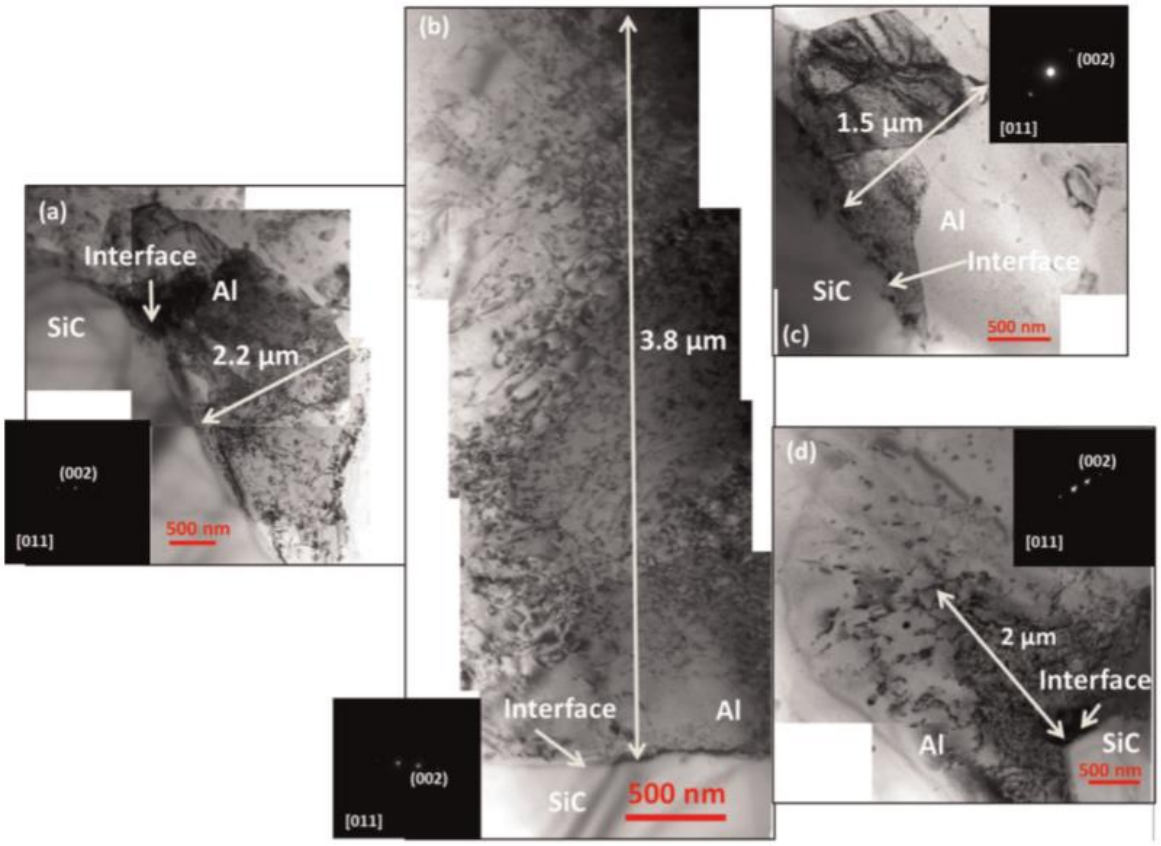

Fig. 19 Transmission electron microscopy (TEM) images of the reinforcement/matrix interface, from SiCp/Al composite samples treated under different processing conditions: (a) as-extruded state; (b) underaged state; (c) peak-aged state; and (d) overaged state (22).

It is very interesting to notice that the simulation results gave a peak stress of over 800 MPa after cooling, which is even larger than the ultimate stress of Al 6061. This is similar to hydrostatic stress which is compressive and concentrated in the thin layer of material in the interface. In the practical field, it is reported that the interface has the least tendency to fail. The interface is very hard and brittle and hence similar to the particles (26, 27), the interface cab considered as an extension of the particle (13). This is likely due to this very high compressive stress in that region.

The finite element analysis by Bouafia et al., (2) showed that lower SiC content lower residual stress and the distribution of SiC particles controls the amount and the gradient of stresses. The scattering and intensity of the stresses are affected by the inter-particle distance and shape of particles.

A larger aspect ratio of the reinforcements makes larger contribution to composite properties (28). The aspect ratio induces directional stress distribution as higher stress is generated in the direction of longer dimension of the reinforcement than that of shorter dimension. In addition, sharp corners of the particles facilitate stress concentration. The smaller the angel of the sharp corners, higher is the stress concentration. As a result of that, no stress concentration was noticed on particles and higher stress concentration occurred on the presence of triangular particles. All these factors are contributed by reinforcement's shapes which induce different patterns of Von-Mises stress along the horizontal line through the matrix and particle. Aspect ratio does not affect the

residual stress noticeably in the case of fibre reinforcements which naturally have very high aspect ratio compare to that of particle reinforcements. This is due to independence of residual fields on axial position at a short distance from fibre corner (11).

The matrix of MMCs tends to shrink in all directions relative to the reinforcements during cooling process. This means, the matrix must extend relative to its stress-free state due to the presence of reinforcements with low CTE to maintain continuity with the reinforcements. This induces tensile residual stress in the matrix and compressive residual stress in the reinforcements and interface. This was confirmed by neutron diffraction technique in SiC whisker-reinforced aluminium matrix composite as reported by Allen et. al. (29). The shape, size and content of reinforced particles affect the extension of matrix and compression of reinforcements as well as the magnitude and distribution of residual stresses (9). Higher elastic modulus of SiC particles induces higher principal residual stress in the particles compare to that of aluminium matrix. Similar conclusions were also experimentally obtained by Coats and Krawitz (20) through neutron diffraction. In addition, Kupperman et al.,(30) used neutron diffraction method to measure the thermal residual stresses in MMCs. Their study indicated that the magnitude of the strains as well as stresses in SiC whisker is much higher in comparison to aluminium matrix.

The residual stress in matrix is in direct relationship with the content of reinforcement, regardless of reinforcement geometry. This indicates that the residual stress is likely to localise at the regions with high particle concentration, if the reinforcement particles are distributed non-homogeneously in the matrix. Therefore, these regions tend to become crack initiation sites, which has significant effects on overall strength of the composites. This result is in good agreement with the findings of Povirk et al., (11)**,** Bouafia et al., (2), and Coats and Krawitz (20). The extent and magnitude of residual stress with the decrease of particle size, when the content of reinforcement remains constant, also agreed with the study of Coats and Krawitz (20).

5. Conclusions

Based on FEA analysis of SiC reinforced aluminium composite with four different geometries of particles, each with three different sizes and three different reinforcement contents, total thirty-six case studies were made for thermal residual stress generated during cooling process from temperature of 582 °C to room temperature of 25 °C. Based on above mentioned result and discussions, following conclusion can be made:

(a) Highest amount of residual stress in the matrix was generated at interface region irrespective of shape, size and content of reinforcements. The effect of size, shape and content of reinforcement on Von-Mises stress becomes noticeable as the distance from the interface increases. A sudden change of stress occurred at matrix/particle interface and an increase/decrease of stress depend on particle shape.

(b) The residual stress in the particle is compressive due to lower thermal expansion coefficient and subsequently causes tensile stress in the matrix. Although the residual stress in the aluminium matrix is mostly in tension with regions of compression stress next to the interface. The directions of the stress vector depends on the shape of the particles and distributed as magnetic field.

(c) The extent of residual stress in matrix increases with decreasing inter-particle spacing, which means increasing reinforcement content or decreasing particle size at constant content. Therefore, the regions with high reinforcement concentration are likely to become crack initiation sites.

(d) Residual stresses are highly dependent on reinforcement geometry which controls the aspect ratio. Maximum von-Mises stress was found for triangular particle reinforced MMCs with decreasing order in rectangular, square and circular particles consequently.

References

1. Paknia A, Pramanik A, Dixit A, Chattopadhyaya S. Effect of Size, Content and Shape of Reinforcements on the Behavior of Metal Matrix Composites (MMCs) Under Tension. Journal of Materials Engineering and Performance. 2016;25(10):4444-59.
2. Bouafia F, Serier B, Bouiadjra BAB. Finite element analysis of the thermal residual stresses of SiC particle reinforced aluminum composite. Computational Materials Science. 2012;54:195-203.
3. Pramanik A, Islam MN, Boswell B, Basak AK, Dong Y, Littlefair G. Accuracy and finish during wire electric discharge machining of metal matrix composites for different reinforcement size and machining conditions. Proceedings of the Institution of Mechanical Engineers, Part B: Journal of Engineering Manufacture. 2016:0954405416662079.
4. Kaczmar J, Pietrzak K, Włosiński W. The production and application of metal matrix composite materials. Journal of Materials Processing Technology. 2000;106(1):58-67.
5. Pramanik A, Basak AK. Effect of machining parameters on deformation behaviour of Al-based metal matrix composites under tension. Proceedings of the Institution of Mechanical Engineers, Part B: Journal of Engineering Manufacture. 2016:0954405416640188.
6. Basak A, Pramanik A, Islam MN, editors. Failure mechanisms of nanoparticle reinforced metal matrix composite. Advanced Materials Research; 2013: Trans Tech Publ.
7. Humphreys F, Miller W, Djazeb M. Microstructural development during thermomechanical processing of particulate metal-matrix composites. Materials Science and Technology. 1990;6(11):1157-66.
8. Hakami F, Pramanik A, Basak AK. Tool wear and surface quality of metal matrix composites due to machining: A review. Proceedings of the Institution of Mechanical Engineers, Part B: Journal of Engineering Manufacture. 2017;231(5):739-52.
9. Ho S, Lavernia E. Thermal residual stresses in metal matrix composites: a review. Applied Composite Materials. 1995;2(1):1-30.
10. Ho S, Saigal A. Three-dimensional modelling of thermal residual stresses and mechanical behavior of cast SiC/A1 particulate composites. Acta metallurgica et materialia. 1994;42(10):3253-62.
11. Povirk G, Needleman A, Nutt S. An analysis of residual stress formation in whisker-reinforced Al · SiC composites. Materials Science and Engineering: A. 1990;125(2):129-40.
12. Teixeira-Dias F, Menezes L. Thermal Residual Stresses in Aluminium Matrix Composites. Heat Transfer in Multi-Phase Materials: Springer; 2010. p. 33-62.
13. Pramanik A, Zhang L, Arsecularatne J. An FEM investigation into the behavior of metal matrix composites: tool–particle interaction during orthogonal cutting. International Journal of Machine Tools and Manufacture. 2007;47(10):1497-506.
14. Pramanik A, Zhang L, Arsecularatne J. Deformation mechanisms of MMCs under indentation. Composites Science and Technology. 2008;68(6):1304-12.

15. Pramanik A, Zhang LC, Arsecularatne JA, editors. Micro-Indentation of Metal Matrix Composite-An FEM Investigation. Key Engineering Materials; 2007: Trans Tech Publ.
16. Pramanik A, Zhang L. Particle fracture and debonding during orthogonal machining of metal matrix composites. Advances in Manufacturing. 2017;5(1):77-82.
17. ASM. Aluminium 6061-T6: Aerospace Specification Metals Inc.; 2017 [cited 2017 26th October]. Available from: http://asm.matweb.com/search/SpecificMaterial.asp?bassnum=ma6061t6.
18. Accuratus. Silicon Carbide, SiC Ceramic Properties: Accuratus Ceramic Corporation; 2017 [cited 2017 26th October]. Available from: http://accuratus.com/silicar.html.
19. Cornwall B, Krstic V. Role of residual stress field interaction in strengthening of particulate-reinforced composites. Journal of materials science. 1992;27(5):1217-21.
20. Coats D, Krawitz A. Effect of particle size on thermal residual stress in WC–Co composites. Materials Science and Engineering: A. 2003;359(1):338-42.
21. Lee EU. Thermal stress and strain in a metal matrix. Metallurgical Transactions A. 1992;23(8):2205.
22. Song J, Guo Q, Ouyang Q, Su Y, Zhang J, Lavernia EJ, et al. Influence of interfaces on the mechanical behavior of SiC particulate-reinforced Al–Zn–Mg–Cu composites. Materials Science and Engineering: A. 2015;644:79-84.
23. Jiptner K, Gao B, Harada H, Miyamura Y, Fukuzawa M, Kakimoto K, et al. Thermal stress induced dislocation distribution in directional solidification of Si for PV application. Journal of Crystal Growth. 2014;408:19-24.
24. Chawla N, Shen Y-L. Mechanical behavior of particle reinforced metal matrix composites. Advanced engineering materials. 2001;3(6):357-70.
25. Lin K, Dai Pang S. The influence of thermal residual stresses and thermal generated dislocation on the mechanical response of particulate-reinforced metal matrix nanocomposites. Composites Part B: Engineering. 2015;83:105-16.
26. Zhu Y, Kishawy H. Influence of alumina particles on the mechanics of machining metal matrix composites. International Journal of Machine Tools and Manufacture. 2005;45(4-5):389-98.
27. Das T, Munroe P, Bandyopadhyay S, Bell T, Swain M. Interfacial behaviour of 6061/AI203 metal matrix composites. Materials science and technology. 1997;13(9):778-84.
28. Zong B, X.-H. G, Derby B. Stiffness of particulate reinforced metal matrix composites with damaged reinforcements. Materials science and technology. 1999;15(7):827-32.
29. Allen AJ, Bourke M, Dawes S, Hutchings M, Withers P. The analysis of internal strains measured by neutron diffraction in Al/SiC metal matrix composites. Acta metallurgica et materialia. 1992;40(9):2361-73.
30. Kupperman D, Majumdar S, MacEwen S, Hitterman R, Singh J, Roberts R, et al. Nondestructive characterization of ceramic composite whiskers with neutron diffraction and ultrasonic techniques. Review of Progress in Quantitative Nondestructive Evaluation: Springer; 1988. p. 961-9.